Electronic Supplementary Material (ESI) for Environmental Science: Nano.

Supplementary Information

for

Traffic-Derived Magnetite Pollution in Soils along a Highway on the Tibetan Plateau

Lin Liu[1,3], Qinghua Zhang[1], Juan Gui[2], Baijuan Zhang[2], Hang Yang[1,3], Dawei Lu[1,3], Zigu Chen[1,3], Qian Liu[1,3,4]*, Zongxing Li[2]*, Guibin Jiang[1,3]

[1] *State Key Laboratory of Environmental Chemistry and Ecotoxicology, Research Center for Eco-Environmental Sciences, Chinese Academy of Sciences, Beijing 100085, China*

[2] *Gansu Qilian Mountains Eco-Environment Research Center, Northwest Institute of Eco-Environment and Resources, Chinese Academy of Sciences, Lanzhou 730000, China*

[3] *College of Resources and Environment, University of Chinese Academy of Sciences, Beijing 100049, China*

[4] *Institute of Environment and Health, Jianghan University, Wuhan 430056, China*

Email: qianliu@rcees.ac.cn (Q. Liu); lizxhhs@163.com (Z. Li)

Contents

3. Supplementary Tables

4. References for SI

1. Supplementary Experimental Section

1.1 Chemicals

Hydrofluoric acid (HF, 40%) and nitric acid (HNO_3, 65%) were purchased from Merck (Darmstadt, Germany). Acetic acid and acetone were purchased from Sinopharm (Shanghai, China). Ultra-pure water (18.3 MΩ·cm) was generated by a MiIIi-Q Gradient system (MiIlipore, Bedford). The multi-element calibration standard solution used for inductively coupled plasma optical emission spectrometer (ICP-OES) detection was purchased from Agilent (Santa Clara, CA). The Pd and Pt calibration standard solutions used for inductively coupled plasma mass spectrometry (ICP-MS) detection were purchased from Guobiao Testing & Certification Co. (Beijing).

1.2 Statistical analysis

We performed independent sample mean tests on different groups of samples. The one-way ANOVA independent-samples T test was used for difference analysis and *P* value calculation. Pearson correlation was used in element correlation analysis, and the two-tailed t-test was employed for *P* value calculation. The statistical analyses were performed using the SPSS Statistics software.

2. Supplementary figures

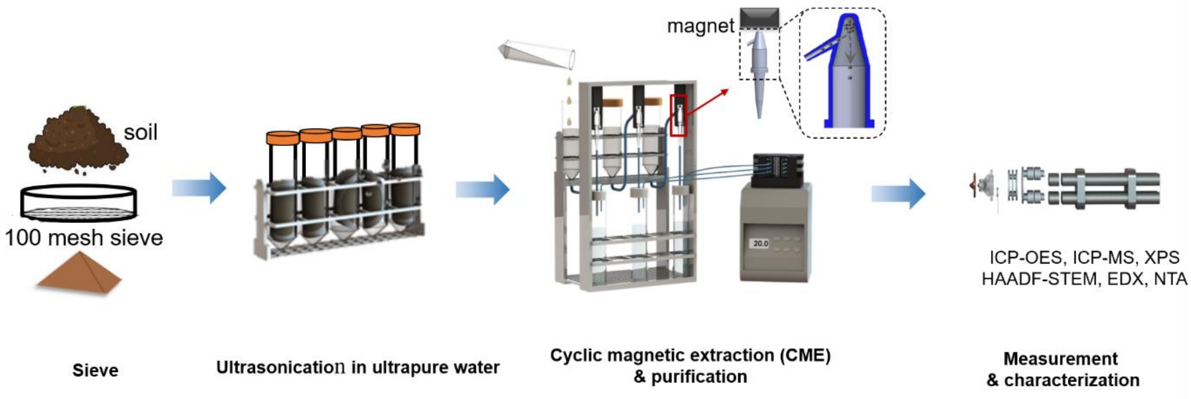

Figure S1. Procedures for sieving, extraction, and analysis of magnetite particles in soils. The method was similar with that established in a previous work by our group[1]. Briefly, the soil samples were first passed through a 100-mesh sieve (sieves are made of stainless steel that does not contain magnetism materials) and then dispersed in an aqueous solution. After that, the magnetic particles were extracted and purified by the CME system. The extracted samples were characterized by HAADF-STEM and quantified by ICP-OES and ICP-MS.

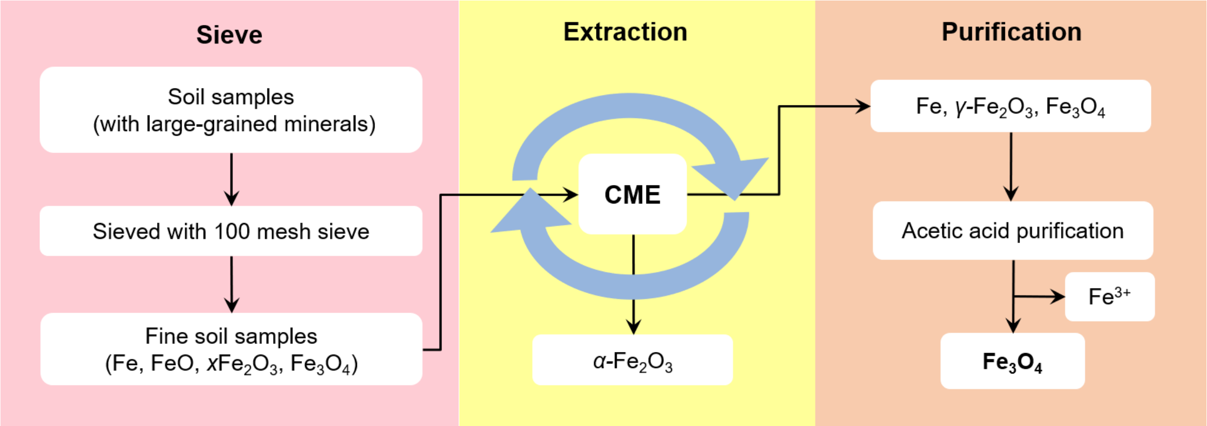

Figure S2. Scheme showing the mechanisms for the sieving, extraction, and purification of magnetite from soils. After the soil sample was sieved, large pieces of natural minerals were removed. The sieved sample was dispersed in ultrapure water and then extracted by the CME system. The extracted sample was purified with acetic acid (2 M) to obtain pure magnetite particles.

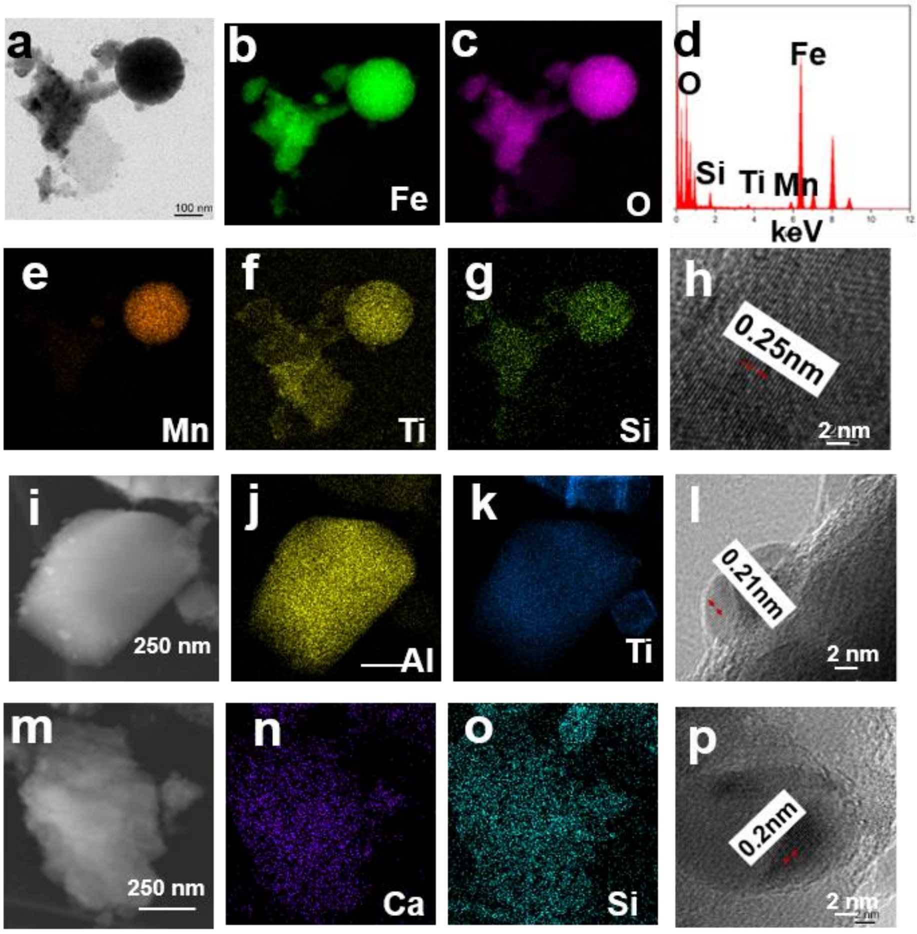

Figure S3. Typical TEM images with elemental mapping analysis of magnetite in the roadside environment. **a**, TEM image of magnetite particles extracted from a roadside soil sample. **b-c**, EDX mapping of Fe and O for the particles in (**a**). **d**, EDXS spectrum of the spherical particles in (**a**). **e-g**, EDX mapping of Mn, Ti, and Si for the particles in (**a**). **h**, Atomic resolution HAADF-STEM image of the spherical particles in (**a**). **i**, HAADF-STEM image of magnetite from the roadside soil with flakey shapes. **j-k**, EDX mapping of Al and Ti for the particles in (**i**). **l**, Atomic resolution HAADF-STEM image of the flaky particles in (**i**). **m**, HAADF-STEM image of magnetite from a roadside soil sample with irregular shapes. **n-o**, EDX mapping of Ca and Si for the particles in (**m**). **p**, HAADF-STEM image of magnetite from roadside soils with irregular shapes.

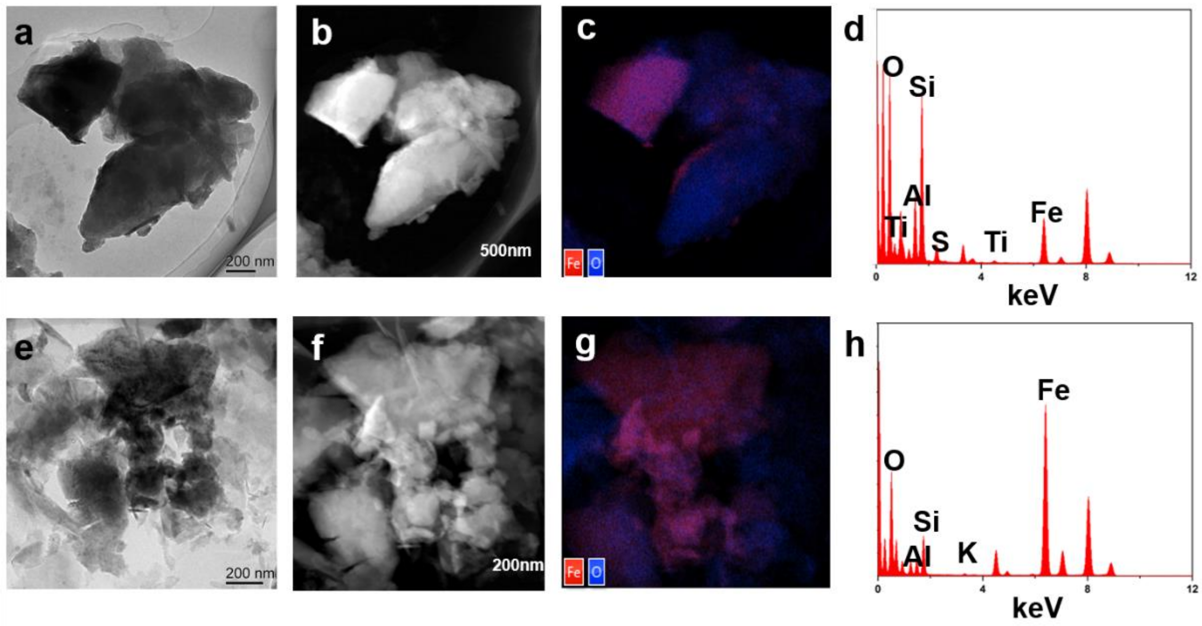

Figure S4. The morphology and elemental distribution characteristics of magnetite particles derived from vehicle emission (a-d) and background soils (e-h). a, TEM image of magnetite particles extracted from traffic source with flaky shapes. **b**, HAADF-STEM image of magnetite in (**a**). **c**, EDX mapping of Fe and O for the particles in (**a**). **d**, EDXS spectrum of the spherical particles in (**a**). **e**, TEM image of magnetite particles extracted from background soils with irregular shape. **f**, HAADF-STEM image of magnetite in (**e**). **g**, EDX mapping of Fe and O for the particles in (**e**). **h**, EDXS spectrum of the spherical particles in (**e**).

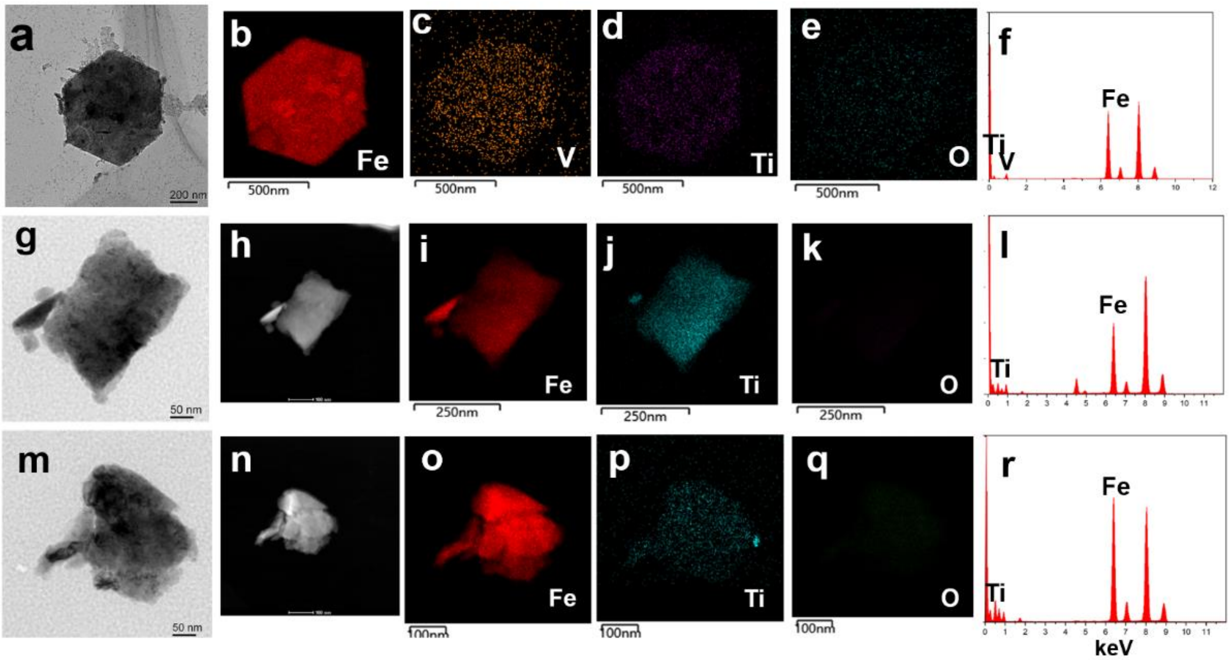

Figure S5. TEM images with elemental mapping and EDX analysis of flaky magnetic particles in the roadside environment consisted of only Fe, Ti, and V. a, TEM image of a magnetite particle extracted from the roadside environment with flaky shape. **b-e**, EDX mapping of Fe, V, Ti, and O for the particle in (**a**). **g**, TEM image of magnetite particles extracted from the roadside environment with flaky shapes. **h**, HAADF-STEM image of magnetite particles in (**g**). **i-k**, EDX mapping of Fe, Ti, and O for the particles in (**g**). **l**, EDXS spectrum of the spherical particles in (**g**). **m**, TEM image of magnetite particles extracted from the roadside environment with flaky shape. **n**, HAADF-STEM image of magnetite particles in (**m**). **o-q**, EDX mapping of Fe, Ti, and O for the particles in (**m**). **r**, EDXS spectrum of the spherical particles in (**m**).

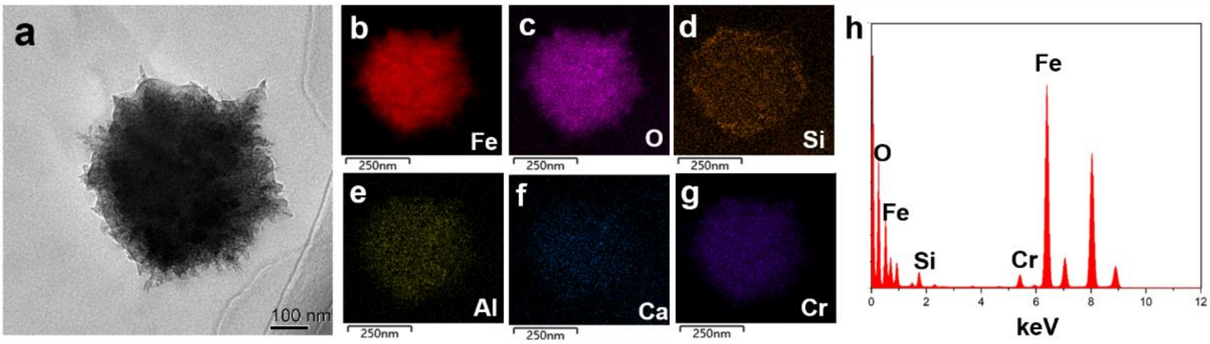

Figure S6. TEM images with elemental mapping of irregular magnetite in the roadside environment. a, TEM image of magnetite particle extracted from the roadside environment with irregular shape. **b-g**, EDX mapping of Fe, O, Si, Al, Ca, and Cr for the particle in (**a**). **h**, EDXS spectrum of the spherical particle in (**a**).

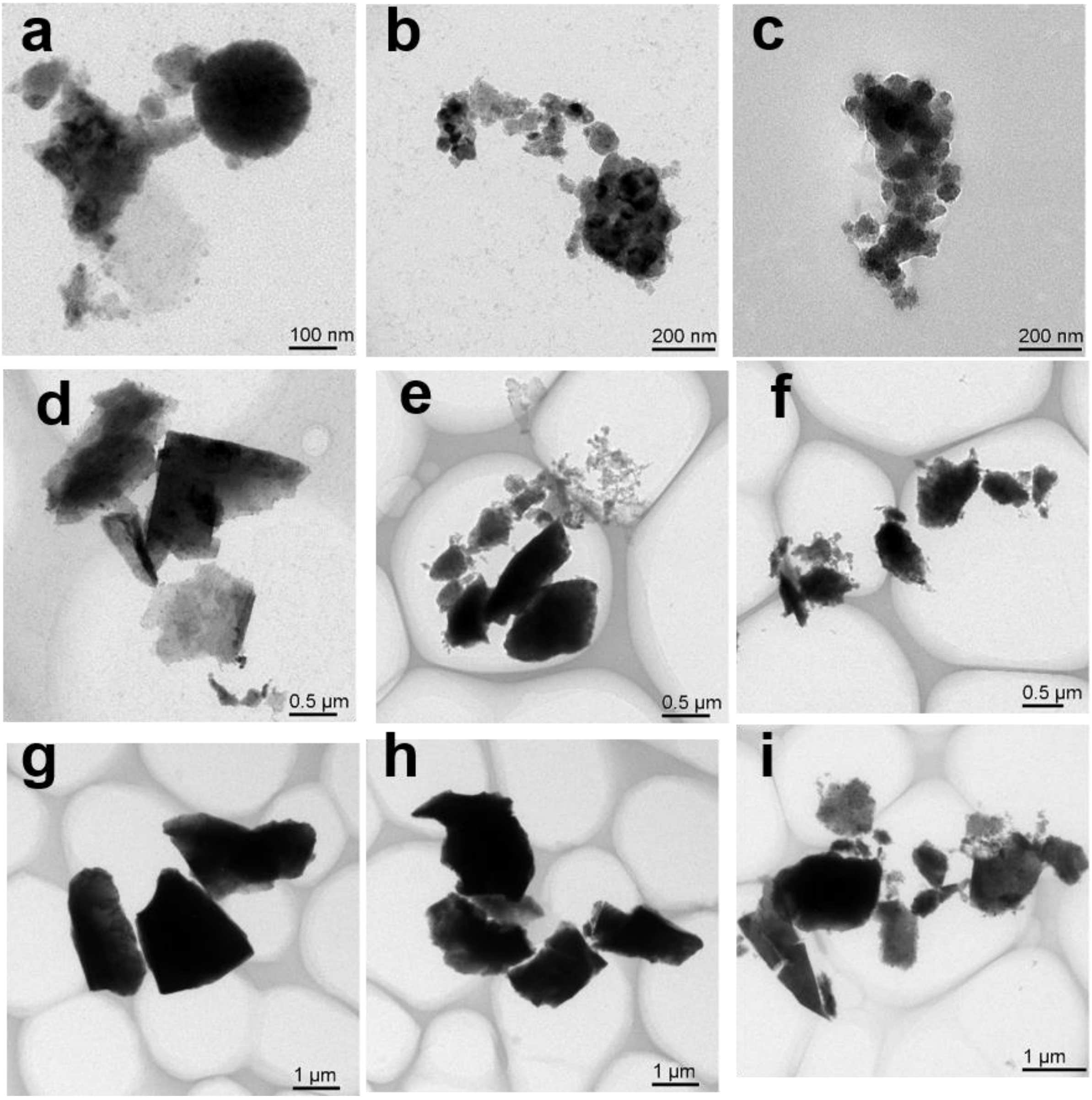

Figure S7. Typical TEM images of magnetite particles extracted from the roadside soils. It can be seen that magnetite particles showed a tendency to form aggregates. Most of them were flaky or irregular in shape, possibly deriving from vehicle wear debris and natural minerals, and only a few were spherical.

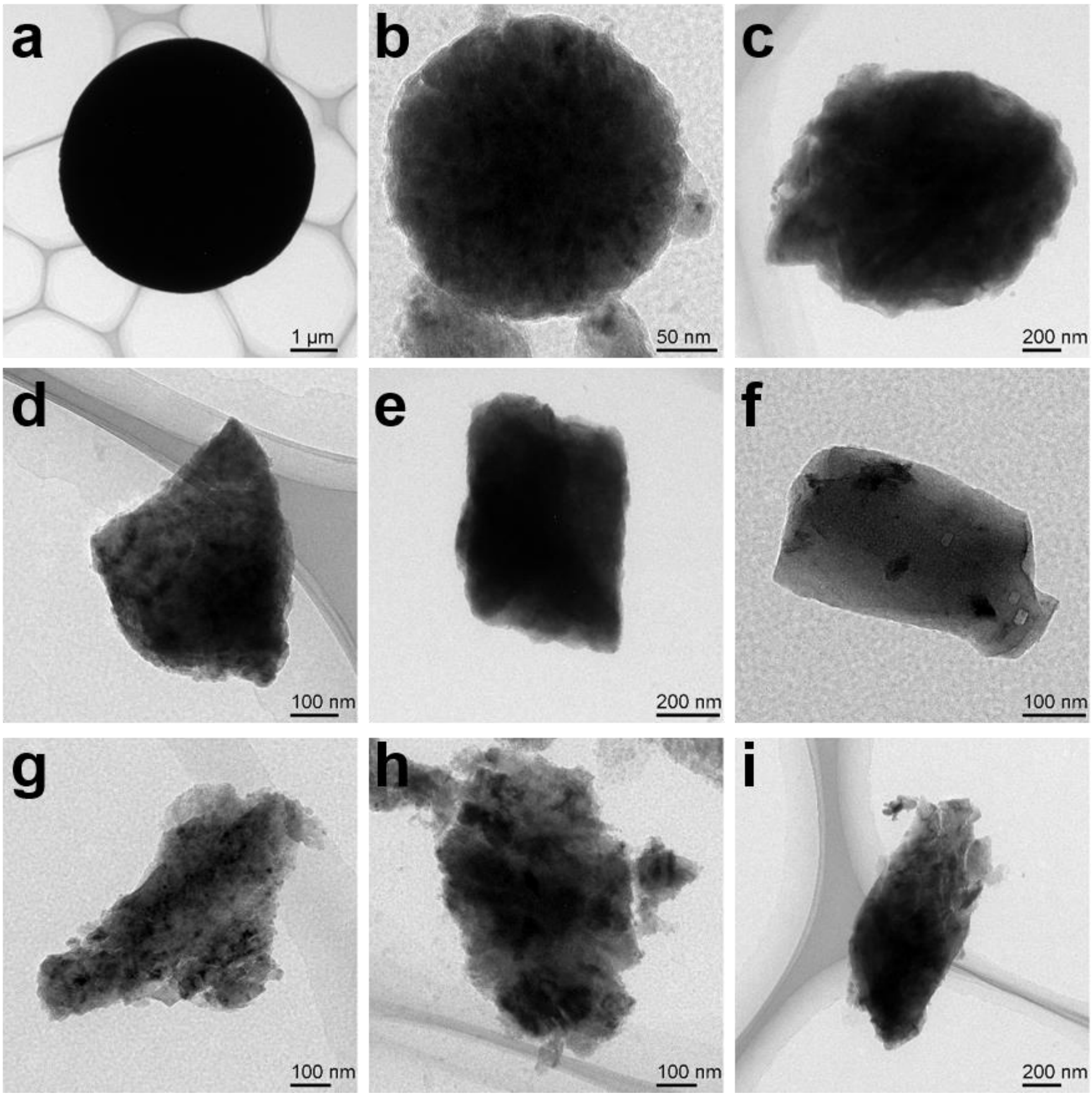

Figure S8. Three different typical morphologies of magnetite particles found in the roadside environment. Magnetite particles mainly had three kinds of morphology, including spherical (**a-c**), flaky (**d-f**), and irregular shapes (**g-i**), and the particle size were mostly less than 1 µm. The spherical and flaky particles mostly had smooth edges, while the irregular particles were rough.

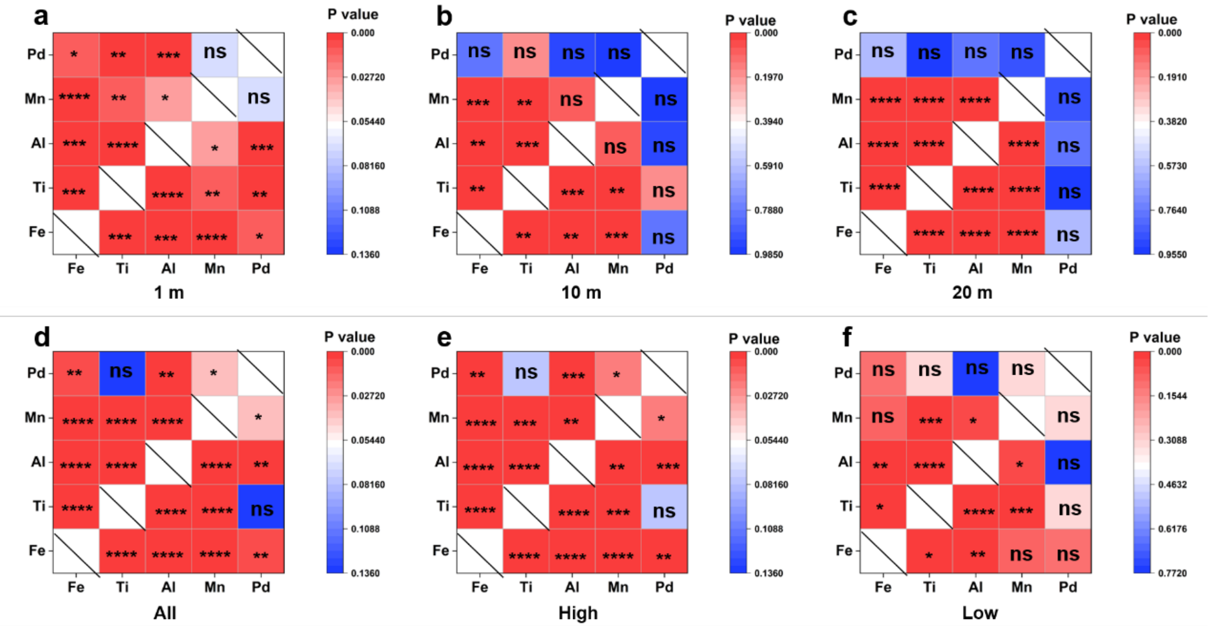

Figure S9. Correlation analysis of different elements in magnetite particles collected in the roadside environment. a, The metal concentrations in the samples collected at 1 m away from road. **b**, The metal concentrations in the samples collected at 10 m away from road. **c**, The metal concentrations in the samples collected at 20 m away from road. **d**, The metal concentrations in all samples. **e**, The metal concentrations in the samples with high-abundance Fe (Fe concentration > 38 ppm). **f**, The metal concentrations in the samples with low-abundance Fe (Fe concentration < 38 ppm). * represents the *p* value of < 0.05, ** represents the *p* value of < 0.01, *** represents the *p* value of < 0.001, **** represents the *p* value of < 0.0001, and ns (no significance) represents the *p* value of > 0.05.

3. Supplementary tables

Table S1. Information of sampling sites.

Site	Longitude	Latitude	Altitude	Point
S1	91.96°E	33.01°N	5072 m	L-1, 10, 20 m; R-1, 10, 20 m; Background-4
S2	91.89°E	33.35°N	4804 m	L-1, 10, 20 m; R-1, 10, 20 m
S3	92.08°E	33.60°N	4700 m	L-1, 10, 20 m; R-1, 10, 20 m
S4	92.32°E	33.82°N	4605 m	L-1, 10, 20 m; R-1, 10, 20 m
S5	92.38°E	34.15°N	4633 m	L-1, 10, 20 m; R-1, 10, 20 m; Background-3
S6	92.66°E	34.38°N	4585 m	L-1, 10, 20 m; R-1, 10, 20 m
S7	92.91°E	34.67°N	5010 m	L-1, 10, 20 m; R-1, 10, 20 m
S8	92.95°E	34.95°N	4559 m	L-1, 10, 20 m; R-1, 10, 20 m; Background-2
S9	93.10°E	35.24°N	4633 m	L-1, 10, 20 m; R-1, 10, 20 m
S10	93.49°E	35.38°N	4487 m	L-1, 10, 20 m; R-1, 10, 20 m
S11	93.88°E	35.52°N	4638 m	L-1, 10, 20 m; R-1, 10, 20 m; Background-1
S12	94.06°E	35.64°N	4781 m	L-1, 10, 20 m; R-1, 10, 20 m

* L represents the left side of the road, and R represents the right side of the road (facing north).

Table S2. Recoveries of magnetic NPs in the spiked soil samples using the CME method.

Sample	Recovery (%; mean ± SD, *n* =3)
Magnetite NPs (10 mg/g)	79.6 ± 7.9
Magnetite NPs (20 mg/g)	83.2 ± 3.7
Magnetite NPs (50 mg/g)	85.5 ± 1.4
Maghemite NPs (20 mg/g)	ND [a]
Zero-valent iron NPs (20 mg/g)	ND [a]

[a] "ND" means that the detection signals showed no significant difference compared with blank samples.

Table S3. The concentration of Fe and accompanied elements (Ti, Al, Mn, Pd, and Pt) in extracted magnetite particles from soil samples.

Site	Fe (μg/g)	Ti (μg/g)	Al (μg/g)	Mn (μg/g)	Pd (pg/g)	Pt (pg/g)
S1L20	4.58×10^{2}	45.1	39.9	1.92	63.6	49.1
S1L10	2.39×10^{2}	26.0	35.8	0.05	57.6	1.05×10^{2}
S1L1	3.25×10^{3}	1.27×10^{2}	2.70×10^{2}	30.5	63.7	13.9
S1R1	2.00×10^{3}	94.2	2.11×10^{2}	19.3	92.0	1.85×10^{2}
S1R10	1.33×10^{3}	64.6	1.21×10^{2}	9.26	76.0	51.8
S1R20	3.87×10^{3}	28.1	38.2	1.38	33.0	1.09×10^{2}
S2L20	6.43×10^{2}	14.2	22.3	4.34	9.37	34.0
S2L10	5.78×10^{2}	21.3	34.7	6.07	55.4	1.93×10^{2}
S2L1	2.24×10^{3}	48.4	1.24×10^{2}	15.2	31.0	1.46×10^{2}
S2R1	2.48×10^{3}	90.8	3.53×10^{2}	20.7	65.2	35.7
S2R10	4.97×10^{2}	27.9	32.5	2.18	9.99	1.44×10^{2}
S2R20	1.18×10^{3}	48.0	69.1	8.34	22.5	94.5
S3L20	7.74×10^{2}	26.5	35.1	1.35	9.96	20.7
S3L10	9.01×10^{2}	41.8	99.6	6.14	49.9	3.61×10^{3}
S3L1	2.53×10^{3}	1.14×10^{2}	3.70×10^{2}	22.07	32.4	3.74×10^{2}
S3R1	3.56×10^{3}	1.15×10^{2}	2.82×10^{2}	26.1	23.0	42.2
S3R10	2.61×10^{3}	68.5	1.54×10^{2}	19.2	51.7	3.73×10^{2}
S3R20	2.78×10^{3}	27.3	37.7	0.53	8.68	3.30×10^{2}
S4L20	6.36×10^{2}	45.9	89.7	3.80	10.3	195
S4L10	1.11×10^{3}	57.8	1.70×10^{2}	6.12	63.7	24.4
S4L1	2.72×10^{3}	1.05×10^{2}	2.38×10^{2}	13.4	28.9	1.16×10^{3}
S4R1	6.73×10^{3}	51.7	1.57×10^{2}	4.18	43.9	61.9
S4R10	2.02×10^{3}	122	305	11.8	37.6	45.2
S4R20	1.13×10^{3}	69.0	1.34×10^{2}	6.32	49.5	2.15×10^{2}
S5L20	7.54×10^{2}	75.1	2.07×10^{2}	6.52	37.6	32.4
S5L10	9.37×10^{2}	56.8	1.34×10^{2}	6.34	2.05×10^{2}	2.40×10^{3}
S5L1	4.31×10^{3}	3.05×10^{2}	1.43×10^{3}	29.6	53.9	2.64×10^{2}

S5R1	2.28×10^{3}	2.26×10^{2}	9.64×10^{2}	20.7	92.4	50.7
S5R10	1.03×10^{3}	78.3	2.74×10^{2}	7.29	1.01×10^{2}	2.08×10^{2}
S5R20	4.68×10^{2}	77.5	99.8	2.76	50.6	3.80×10^{2}
S6L20	1.17×10^{3}	2.01×10^{2}	6.51×10^{2}	12.8	21.5	816
S6L10	1.70×10^{3}	3.44×10^{2}	1.13×10^{3}	17.5	27.4	26.5
S6L1	1.99×10^{3}	2.98×10^{2}	9.11×10^{2}	16.5	43.8	1.07×10^{2}
S6R1	4.11×10^{3}	4.40×10^{2}	1.77×10^{3}	30.6	63.0	1.47×10^{2}
S6R10	2.75×10^{3}	2.70×10^{2}	9.54×10^{2}	17.1	20.9	1.86×10^{2}
S6R20	2.32×10^{3}	3.81×10^{2}	6.85×10^{2}	19.4	43.7	3.25×10^{2}
S7L20	2.94×10^{2}	66.4	78.7	2.49	12.8	125
S7L10	9.57×10^{2}	79.6	1.86×10^{2}	5.32	24.9	21.7
S7L1	2.19×10^{3}	2.86×10^{2}	1.05×10^{3}	23.6	1.14×10^{2}	55.3
S7R1	8.54×10^{2}	1.02×10^{2}	2.79×10^{2}	6.88	52.6	44.1
S7R10	1.20×10^{3}	90.7	2.20×10^{2}	9.93	93.5	9.02×10^{3}
S7R20	4.97×10^{2}	74.5	118	5.65	44.6	526
S8L20	1.48×10^{2}	16.1	33.8	0.55	66.8	4.20×10^{2}
S8L10	7.33×10^{2}	42.4	39.4	4.07	26.6	12.7
S8L1	2.81×10^{2}	15.9	23.7	ND[a]	42.1	2.30×10^{2}
S8R1	2.33×10^{2}	30.1	16.5	ND	ND	31.8
S8R10	1.93×10^{2}	7.66	17.3	ND	ND	2.75×10^{2}
S8R20	6.95×10^{2}	37.9	54.8	3.27	5.64	20.4
S9L20	5.42×10^{2}	1.71×10^{2}	73.9	7.26	36.2	1.65×10^{3}
S9L10	4.99×10^{2}	91.4	51.6	4.26	18.8	26.1
S9L1	1.63×10^{3}	91.9	1.23×10^{2}	18.8	22.1	2.51×10^{3}
S9R1	3.35×10^{3}	1.83×10^{2}	3.72×10^{2}	64.9	69.4	52.0
S9R10	1.84×10^{3}	2.57×10^{2}	1.47×10^{2}	37.3	35.8	1.12×10^{2}
S9R20	7.44×10^{2}	70.4	60.8	11.5	17.6	2.67×10^{2}
S10L20	3.25×10^{2}	66.3	62.7	2.50	19.6	3.22×10^{2}
S10L10	7.69×10^{2}	1.15×10^{2}	1.18×10^{2}	13.7	1.01×10^{2}	1.35×10^{2}

S10L1	6.52×10^{2}	88.8	1.34×10^{2}	8.63	30.0	1.39×10^{2}
S10R1	1.95×10^{3}	81.2	1.42×10^{2}	21.9	13.4	1.79×10^{2}
S10R10	6.63×10^{2}	1.07×10^{2}	79.8	13.6	28.6	22.4
S10R20	6.51×10^{2}	1.48×10^{2}	83.4	14.5	57.6	5.65×10^{2}
S11L20	3.15×10^{2}	57.8	47.5	1.53	8.05	65.5
S11L10	2.29×10^{2}	1.04×10^{2}	65.8	3.42	24.9	13.6
S11L1	5.21×10^{2}	85.5	38.8	2.51	45.6	1.29×10^{2}
S11R1	6.97×10^{2}	83.5	73.7	4.18	7.96	66.9
S11R10	1.30×10^{3}	3.74×10^{2}	1.06×10^{2}	11.8	13.3	73.0
S11R20	3.63×10^{2}	89.5	67.5	3.79	9.17	1.56×10^{2}
S12L20	4.97×10^{2}	99.3	80.61	5.88	18.7	56.1
S12L10	5.31×10^{2}	90.0	79.54	4.38	45.5	77.1
S12L1	2.39×10^{2}	77.5	52.65	7.20	16.9	73.9
S12R1	9.70×10^{2}	56.5	40.35	6.43	20.6	1.15×10^{2}
S12R10	9.88×10^{2}	85.3	66.82	12.1	35.2	28.4
S12R20	3.50×10^{2}	62.6	52.41	2.23	49.4	2.90×10^{2}
control1	1.75×10^{2}	19.7	14.1	ND	227	84.3
control2	2.67×10^{2}	31.7	33. 3	ND	59.6	50.9
control3	6.34×10^{2}	49.3	58.8	1.31	41.6	73.3
control4	2.44×10^{2}	19.2	18.4	ND	67.4	24.8

[a] “ND” means that this element was not detected in the sample.

Table S4. Abundance of magnetite particles in the roadside soils (mg/g).

	L20 m	L10 m	L1 m	R1 m	R10 m	R20 m	Background
S1	0.63	0.33	4.48	2.77	1.84	0.54	0.34
S2	0.89	0.80	3.10	3.43	0.68	1.63	
S3	1.07	1.25	3.49	4.92	3.60	0.385	
S4	0.88	1.54	3.76	0.93	2.80	1.57	
S5	1.04	1.30	5.96	3.15	1.42	0.65	0.88
S6	1.62	2.36	2.76	5.68	3.80	3.21	
S7	0.41	1.32	3.03	1.18	1.66	0.69	
S8	0.21	1.01	0.39	0.32	0.27	0.96	0.37
S9	0.75	0.69	2.25	4.63	2.54	1.03	
S10	0.45	1.06	0.90	2.70	0.92	0.90	
S11	0.44	0.32	0.72	0.96	1.80	0.50	0.24
S12	0.69	0.73	0.33	1.34	1.37	0.48	

* L20 m represents the soil sample at 20 m to the left of the road edge (facing north), R20 m represents the soil sample at 20 m to the right of the road edge (facing north). Similar for L10 m, L1 m, R 1m, and R10 m. “Background” means the background control samples located in more than 450 m from roadside.

Table S5. The *p* values for the comparison of concentration of magnetite particles in soils collected at different distances away from roadside.

	1 m vs. 10 m	10 m vs. 20 m	20 m vs. background	1 m vs. 10 and 20 m
p value	0.006	0.018	0.181	< 0.001
Significant	Yes	Yes	No	Yes

The one-way ANOVA Independent-samples T test was used.

Table S6. Contribution of anthropogenic sources of magnetite particles in the roadside soils (%).

	L20 m	L10 m	L1 m	R1 m	R10 m	R20 m
S1	50.1	4.2	93.0	88.6	82.8	40.9
S2	64.4	60.4	89.8	90.8	53.9	80.6
S3	70.4	74.6	90.9	93.6	91.2	17.7
S4	64.0	79.5	91.6	66.0	88.7	79.8
S5	69.6	75.6	94.7	90.0	77.8	51.1
S6	80.5	86.6	88.5	94.4	91.7	90.1
S7	22.1	76.1	89.5	73.2	81.0	54.0
S8	0[a]	68.8	18.5	1.6	0[a]	67.1
S9	57.8	54.1	86.0	93.2	87.5	69.2
S10	29.6	70.2	64.9	88.3	65.5	64.8
S11	27.3	0.2	56.1	67.2	82.4	37.0
S12	54.0	56.9	4.2	76.4	76.8	34.7

* L20 m represents the soil sample at 20 m to the left of the road edge (facing north), R20 m represents the soil sample at 20 m to the right of the road edge (facing north). Similar for L10 m, L1 m, R 1m, and R10 m. "Background" means the background control samples located in more than 450 m from roadside.

[a] "0" means that the concentration of magnetite particles in this sample is lower than background value.

Table S7. Correlation analysis between the concentration of iron and other elements in all samples.

	Fe vs. Ti	Fe vs. Al	Fe vs. Mn	Fe vs. Pd
Pearson r	0..6316	0.7186	0.8305	0.3062
p value	<0.0001	<0.0001	<0.0001	0.0075
Significant	Yes	Yes	Yes	Yes

The two-tailed Pearson correlation analysis was used.

Table S8. Correlation analysis between the concentration of iron and other elements in samples 1 m away from roadside.

	Fe vs. Ti	Fe vs. Al	Fe vs. Mn	Fe vs. Pd
Pearson r	0.6618	0.6715	0.7994	0.5180
p value	0.0004	0.0003	<0.0001	0.0113
Significant	Yes	Yes	Yes	Yes

The two-tailed Pearson correlation analysis was used.

Table S9. Correlation analysis between the concentration of iron and other elements of samples in the high-Fe-abundance group.

	Fe vs. Ti	Fe vs. Al	Fe vs. Mn	Fe vs. Pd
Pearson r	0.5477	0.6586	0.7611	0.4220
p value	<0.0001	<0.0001	<0.0001	0.0028
Significant	Yes	Yes	Yes	Yes

The two-tailed Pearson correlation analysis was used.

Table S10. Correlation analysis between the concentration of iron and other elements of samples in the low-Fe-abundance group.

	Fe vs. Ti	Fe vs. Al	Fe vs. Mn	Fe vs. Pd
Pearson r	0.4615	0.4883	0.3772	0.3186
p value	0.0134	0.0084	0.0836	0.1127
Significant	Yes	Yes	Yes	No

The two-tailed Pearson correlation analysis was used.

References for SI

1. Q. H. Zhang, D. W. Lu, D. Y. Wang, X. Z. Yang, P. J. Zuo, H. Yang, Q. Fu, Q. Liu and G. B. Jiang, Separation and Tracing of Anthropogenic Magnetite Nanoparticles in the Urban Atmosphere, *Environ. Sci. Technol.*, 2020, **54**, 9274-9284.